FINAL TECHNICAL REPORT

Time-dependent creep of the Calaveras fault from 18-years of InSAR, GPS and repeating earthquakes

Award Number:	**G13AP00035**
Start Date & End Date:	6/2013 – 5/2014
Principal Investigator:	Roland Bürgmann
Email Address:	burgmann@seismo.berkeley.edu
Co-Principal Investigator:	Ingrid Johanson
Email Address:	ingrid@seismo.berkeley.edu
Co-Principal Investigator:	Robert Nadeau
Email Address:	nadeau@seismo.berkeley.edu
Institution and Address:	University of California, Berkeley
	Berkeley Seismological Laboratory
	215 McCone Hall # 4760
	Berkeley, CA 94720-4760

Abstract

We present the results of our efforts to analyze and model two decades of regional crustal deformation data in the San Francisco Bay region, with a focus on investigating time dependent processes the Calaveras fault. This project builds on progress made during several years of NEHRP funded research and addresses the seismic potential and natural hazard presented by a major fault in the San Francisco Bay Area through the use of space geodesy. Geodetic measurements provide information on the nature of elastic strain accumulation about seismogenic faults, their locking depth and slip rates, and any variations of those parameters in space and time due to time-dependent deformation processes.

Imaging strain accumulation about faults with sufficient precision and spatio-temporal resolution is a difficult task, plagued especially by limits in the accuracy and spatial density of the surface measurements. This project incorporates time series processing of InSAR data spanning 18 years, together with 17 years of GPS acquisitions processed in a consistent manner to form BAVU3. The more sparsely distributed, but continuously operating CGPS BARD and PBO networks provide a precise geodetic backbone with high temporal resolution into which we integrate campaign-mode measurements collected by our and other groups, including the USGS. Additionally, we have expanded the catalog of characteristically repeating earthquakes (CREs) into the southern Calaveras fault and push the detection limit to smaller magnitude repeaters.

Reducing losses from earthquakes. The project contributes improved estimates of earthquake potential on the Calaveras fault by constraining rates of strain accumulation and rates and variability of fault creep. The continuity of fault slip through the stepover between the Hayward and Calaveras faults suggests that rupture scenarios involving both faults should be fully incorporated in earthquake hazard estimates.

Time-dependent creep of the Calaveras fault from 18-years of InSAR, GPS and repeating earthquakes

Award Number: **G13AP00035**

Roland Bürgmann

Ingrid Johanson

Robert Nadeau

University of California, Berkeley

Berkeley Seismological Laboratory

215 McCone Hall # 4760

Berkeley, CA 94720-4760

Telephone: (510) 643-9545;

Fax:(510) 643-5811;

E-mail: burgmann@seismo.berkeley.edu

This project addresses the seismic potential and natural hazard presented by the Calaveras fault in the Eastern San Francisco Bay Area through the use of space-geodetic surface deformation measurements enhanced by constraints from the distribution of repeating microearthquakes in space and time. We build on progress made during several years of NEHRP funded research, this time focusing on the spatiotemporal variation of creep on the Calaveras fault to better resolve the distribution of locked rupture asperities and to resolve temporal variations in aseismic fault slip rates along this urban fault. Geodetic measurements provide information on the nature of elastic strain accumulation about seismogenic faults, their locking depth and slip rates, and any variations of those parameters in space and time due to time-dependent processes. These data, collected by many groups, have been used in a large number of studies aimed at a better understanding of the nature and rates of active strain accumulation in the Bay Area [e.g. *Murray and Segall*, 2001; 2001; *Prescott et al*., 2001; *Parsons*, 2002; *Manaker et al*., 2003; *Pollitz*, 2004; *Pollitz and Nyst*, 2004; *Savage*, 2004; *d'Alessio et al*., 2005; *Johanson and Bürgmann*, 2005; *Schmidt et al*., 2005; *Bürgmann et al*., 2006; *Johanson et al*., 2006; *Johnson*, 2006; *Funning et al*., 2007; *Ryder and Bürgmann*, 2008; *Jolivet et al*., 2009; *Shirzaei and Bürgmann*, 2013]. These studies improved our estimates of slip rates on individual faults, the distribution of locked and creeping segments at depth, and the role of viscous processes at depth in the evolution of active deformation through the earthquake cycles of Bay area faults.

Assessment of earthquake potential along Bay Area faults is complicated by the recognition that the system is not static, but rather strain rates vary through time in response to a variety of phenomena. These can range from the small and quick, such as slow slip events (SSEs) to the large and protracted, such as viscous relaxation following the 1989 Loma Prieta or 1906 San Francisco earthquakes (e.g., *Kenner and Segall,* 2003, *Pollitz et al.,* 1998; *Pollitz and Nyst*, 2005). Time-variable strain affects hazard estimates in three ways. First, it changes our estimate of a fault's slip budget when we realize that strain accumulation and creep rates are not steady over the entire earthquake cycle. Secondly, time-variable strain introduces changes in stress rate on individual fault segments that could have consequences for earthquake timing either through stress shadowing or event triggering (*Pollitz and Nyst*, 2005). Finally, characterizing the kinematics of time variable strain and fault slip leads to better constraints on earth structure and fault frictional parameters, which inform a variety of models, from those spanning multiple earthquake cycles to dynamic rupture models.

The Calaveras fault lies near major urban areas in the San Francisco Bay region, including San Jose, Fremont, and the cities of the San Ramon Valley corridor and has the potential to cause significant loss of life and property. Since 1850, there have been 13 earthquakes of M_L 5 or greater on or near the Calaveras fault (*Oppenheimer et al*., 1990). Calaveras fault monitoring by GPS, creepmeter, gravity, magnetic and seismic data suggest a connection to the Hayward fault and active creep along much of the fault trace (*Ponce et al*., 2004; *Manaker et al*., 2005). The theodolite triangulation method also detected variations in creep rate on the southern Calaveras fault following the Loma Prieta earthquake (*Galehouse*, 1990). Furthermore, investigation of the distribution of seismicity along the fault reveals that in regions where $M_L > 5$ earthquakes occur, little seismicity above M_L 1.4 is found and that pre-mainshock and aftershock microseismicity patterns are similar (*Oppenheimer et al*., 1990). The spatial and temporal variability of the creeping and seismic behavior of the Calaveras suggest that the situation at depth is more complicated than a single locked/creeping region, leading to a time-dependent hazard for the Bay Area.

Under this project, we have extended our analysis of transient slip on East Bay Area faults, funded under NEHRP FY11 and FY12, which includes processing 18 years of InSAR data into an advanced multitemporal InSAR scheme, updating the GPS data and expanding and updating the catalog of characteristically repeating earthquakes (CREs) on the Calaveras fault, extending it further along the southern Calaveras fault and to smaller earthquakes.

A) Geodetic Monitoring of Active Bay Area Deformation

Imaging strain accumulation about faults with sufficient precision and spatiotemporal resolution is a difficult task, plagued especially by limits in the accuracy and spatial density of the surface measurements. GPS and InSAR have been important additions to the geodesist's toolset for nearly two decades. The length of these observations and the continually growing dataset mean that we can detect more subtle and longer-term variations from the secular deformation rates. GPS, InSAR and CREs are highly complimentary data types; each provides a feature the others cannot. GPS has been the primary tool for crustal deformation measurements in the Bay Area since the early 1990s, providing mm-level precise measurements of motion in three dimensions at a relatively sparse number of locations. InSAR data provide dense spatial coverage, which makes them particularly valuable for resolving fine-scale deformation features and vertical motions, though by themselves interferograms provide only one dimension of motion (range change). Where GPS and InSAR are surface measurements and provide information on fault slip

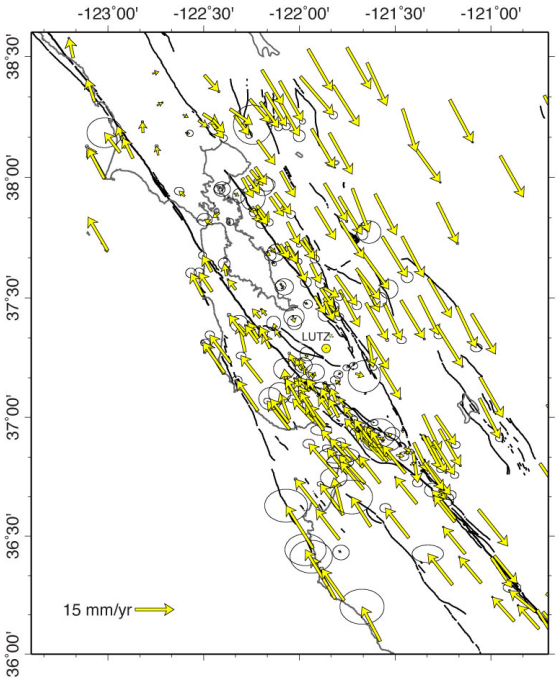

Figure 1a. *BAVU3beta version of San Francisco Bay Area velocities derived from curve fitting to individual time series. All velocity vectors are plotted relative to station LUTZ, on the Bay block.*

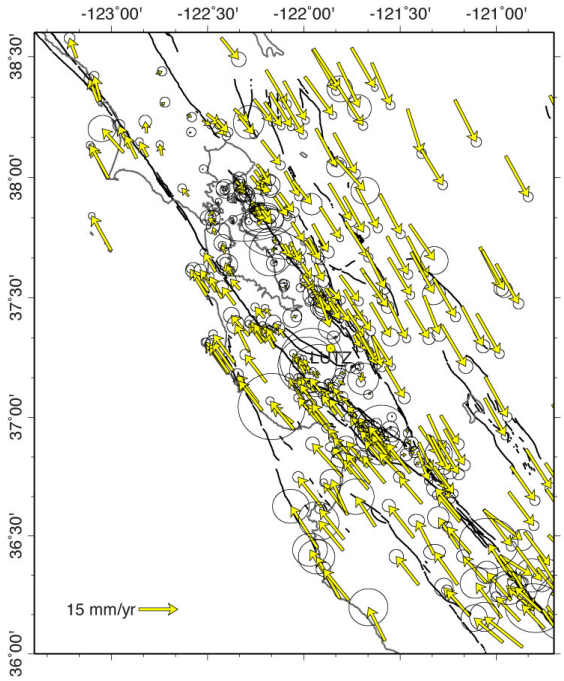

Figure 1b. *Final BAVU3 velocities determined using GLOBK. Velocities were stabilized in the ITRF2008 reference from and then transformed to be relative to station LUTZ.*

at depth through the filter of the Earth's crust, CREs provide direct measurements of creep at depth at their precise location on the fault. InSAR range-change data, in conjunction with GPS surface velocities and the distribution and rate of CREs, have been used to estimate the creep distribution on the upper 12 km of the Hayward fault using dislocation modeling (e.g. *Bürgmann et al*., 2000; *Schmidt et al*., 2005; *Funning et al*., 2005; *Shirzaei and Bürgmann*, 2012a). Improved InSAR processing techniques for producing time series from large sets of interferograms (e.g., *Ferretti et al*., 2004, *Berardino et al*., 2002, *Shirzaei*, 2012b; *Shirzaei and Bürgmann*, 2012a) allow for better coverage alongside Bay area faults and improve our ability to determine the subsurface slip distribution when combined with GPS, and eventually CRE, velocities.

Continuous and Campaign GPS Data. Given the time span and spatial resolution, InSAR data play the key role in our analysis. However, this project made use of both secular velocities and time series for continuous GPS stations and secular velocities of sites observed by episodic campaigns. Three major categories of data exist for the Calaveras fault region: long time-span continuous data (mostly BARD sites, as well as US Coast Guard), more recent PBO continuous data, and campaign data. While campaign data does not have the time sampling to robustly constrain time-varying fault slip, sites with repeated observations over a long time span can nonetheless be used to constrain the cumulative velocity field as part of the Bay Area Velocity Unification (BAVU). Likewise, while more recent PBO (and other) stations do not have data to constrain variability in the early portion of the study period, they can contribute to the secular slip field as well as the later portion.

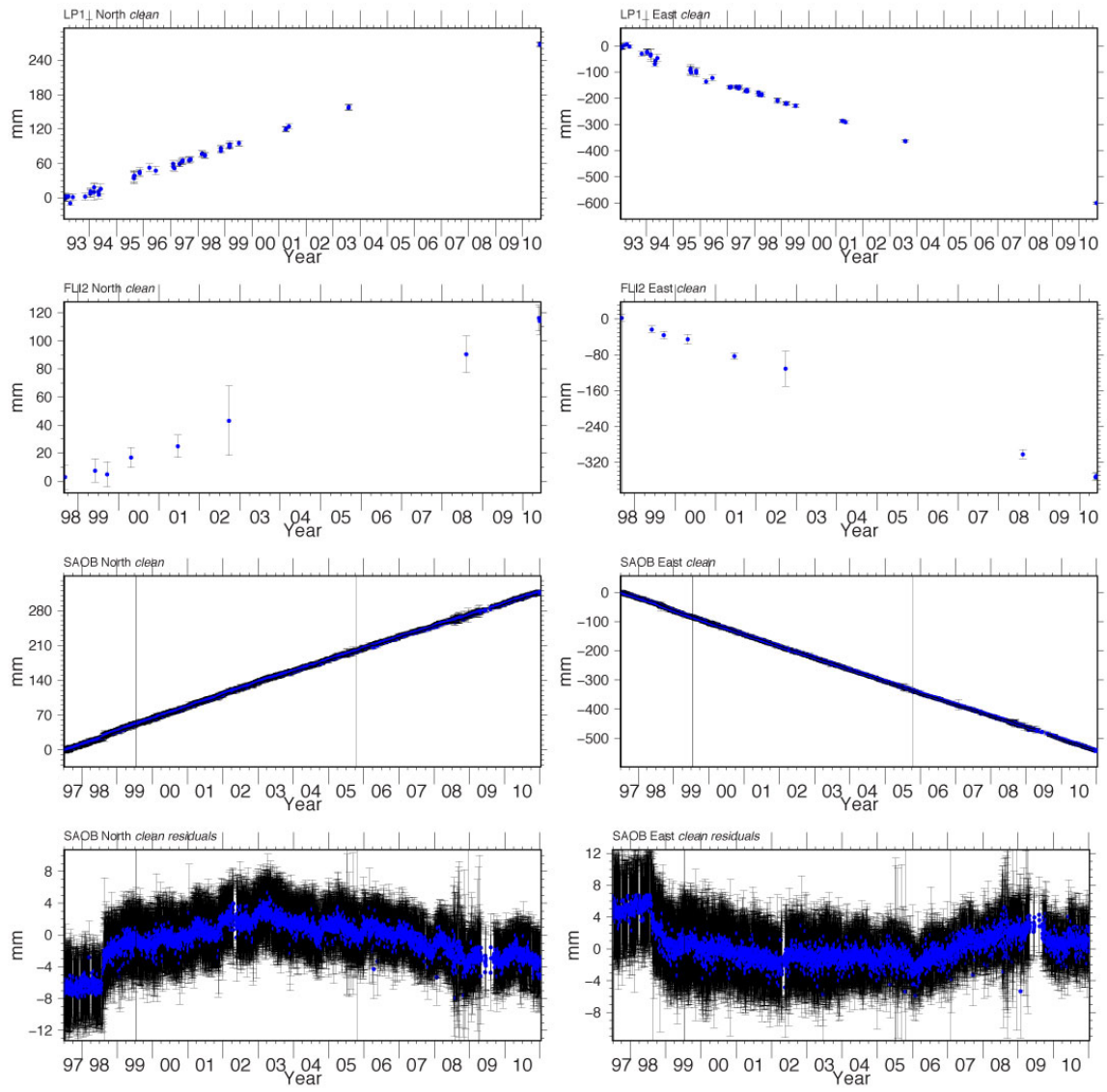

Figure 1c. *Top two lines are example time series of campaign sites in the South Bay and East Bay areas. The time series show motion in the ITRF2008 reference frame. The bottom two lines show the motion of continuous station SAOB in the South Bay Area. The third line is SAOB in the ITRF2008 reference frame and the fourth line is the detrended time series for the same station. After detrending, transient motion, such as offsets from a M518 earthquake in 1998 and the following postseismic motion are more readily apparent.*

BAVU is a mix of campaign mode GPS measurements and data from continuously operating GPS stations (Figure 1). The sparsely distributed, but continuously operating BARD and PBO networks provide a precise 3D geodetic framework with high temporal resolution. Repeated campaign GPS measurements in the Bay Area by our group, the USGS, and others, provide densification. Figures 1a and 1b compare the BAVU3β velocity field with the final BAVU3 results. BAVU3β was generated by fitting slopes to individual station time series (e.g. Figure 1c), while BAVU3 was produced using GLOBK to estimate and stabilize the velocities in a global refer-

ence frame (ITRF2008). Although more data was included in BAVU3, the differences are otherwise minor. The comparison nonetheless provides a useful check on how well constrained the resultant velocities are.

B) Characterizing interseismic creep and stress accumulation on the Calaveras fault using InSAR

An evaluation of interseismic strain accumulation and creep traditionally relies on GPS, alignment arrays and creepmeters, providing precise, but only horizontal and spatially sparse measurements. Here, we use InSAR to resolve small-amplitude long and short-wavelength displacements associated with the Calaveras interseismic deformation and validate our velocity field using BAVU3 GPS and alignments arrays data.

To obtain a 2D velocity field of creep and stress accumulation rates on the Calaveras Fault we must first overcome two challenges. First, InSAR remains rarely used to characterize long wavelength signal. The reason behind being that long wavelength noise (ramps), often considered as resulting from orbital errors, was considered larger than the expected interseismic deformation. However, recent works have demonstrated that when combining tens to hundreds of SAR acquisitions in forms of time series analysis the orbital accuracy of SAR satellites enable detection of long-wavelength deformation > 1.5 mm/yr/100 km (Table 1) (Fattahi and Amelung, 2014).

Satellite	Horizontal orbit uncertainty (cm)	Vertical orbit uncertainty	Acquisitions per year	Total time (yrs)	Ramp in range (mm/yr/100km)	Ramp in azimuth
ERS	12	2	6	8	1.4	1.5
Envisat	4	2	6	8	0.5	0.9

Table 1: *Amplitude of the orbital ramps for the 2 SAR satellites used.*

To resolve the 1992-2011 interseismic ground deformation in the Bay Area we perform an InSAR time-series analysis of ERS and Envisat data. We rely on multiple viewing geometries (ascending and descending) to isolate vertical and horizontal deformation (Wright et al., 2004) and processed a total of 1200 interferograms on 4 tracks and 6 frames (Table 2 and Figure 2) provided through the WInSAR archive.

Path	Frame	Beam	ERS	Env	Igrams	Time
70	2853	Desc	75	31	302	92-11
299	2853	Desc	75	23	488	92-11
206	747	Asc	0	25	131	03-10
206	729	Asc	0	27	92	03-10
478	747	Asc	29	22	115	95-11
478	729	Asc	19	13	48	01-11

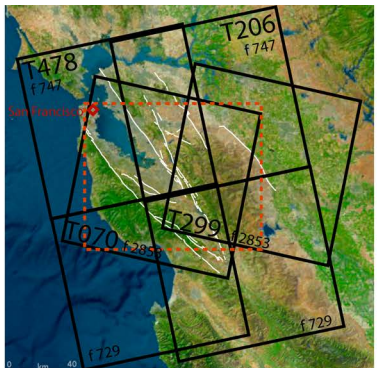

Table 2 and Figure 2: *SAR data processed to produce a 2D InSAR velocity field.*

Our second challenge is to maintain coherence across the Calaveras fault despite the sharp transition from urban areas from vegetated hillslopes. We developed an alternative Small Baseline Subset time series method, in which the image-pair selection is based on the percentage of coherent pixels in each interferogram in an area that spans the fault (black rectangle on the bottom row of Figure 3). Figure 3 shows that the correlation-based selection leads to temporal coherence of 0.6-0.7 on the eastern side of Calaveras compared to values of 0.3-0.4 in typical SBAS. Thus, the advantage of this method is that high spatial coverage is maintained across the fault (temporal coherence >0.5), enabling evaluation of creep and stress accumulation rates. The inconvenient is that some SAR acquisitions must be discarded due to low coherence in the vegetated side of the Calaveras Fault, leading to a lower temporal sampling (Figure 3 top rows).

To validate the InSAR velocity field obtained from this method we compare adjacent tracks, compare horizontal InSAR velocities with the BAVU3 GPS velocities, and compare InSAR time-series with alignment arrays, and creepmeter measurements.

InSAR results

Our InSAR velocity maps provide the first estimates of creep and stress accumulation of the Calaveras fault thanks to the correlation based selection (Figure 4). Additionally, because we do not remove any ramps in our processing (except for a Local Oscillator Drift Correction applied to Envisat data following Marinkovic and Larsen (2013)) our velocity field does not require alignment to an a priori model of deformation based on GPS data. This differs from previous works looking at interseismic deformation in the Bay Area in which long-wavelength signal was con-

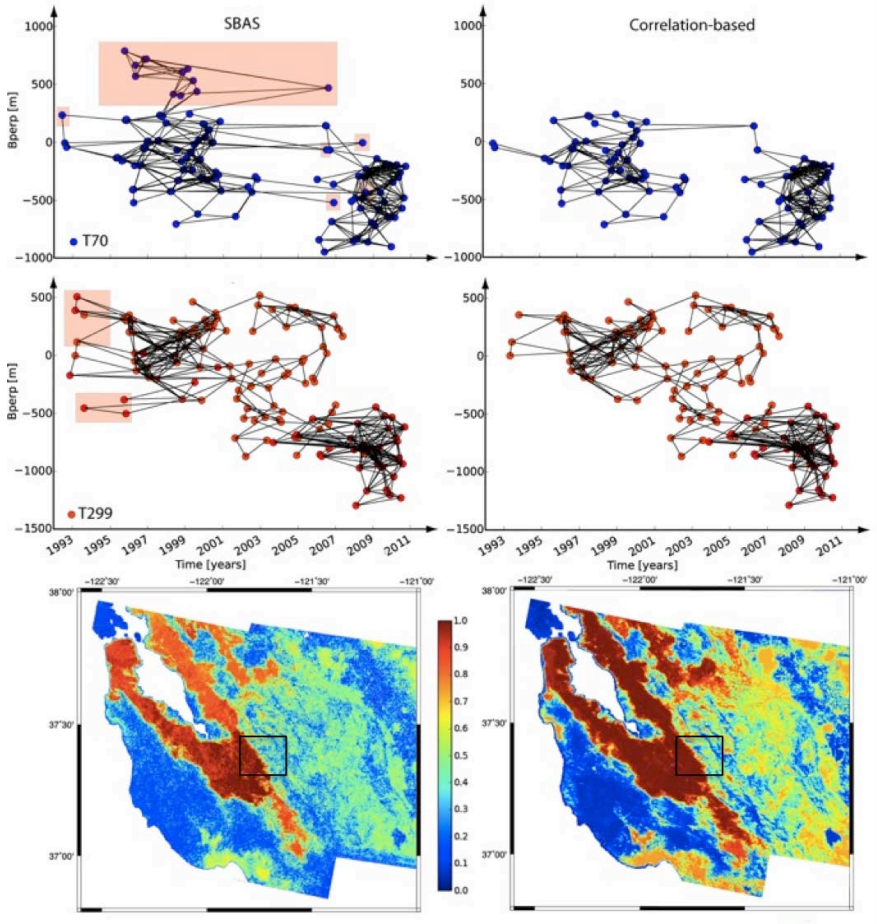

Figure 3: *Typical SBAS network and temporal coherence (left) compared to SBAS with interferograms selection based on correlation (right). Top: perpendicular versus temporal baselines plots for track 70; middle: same for track 299. Red areas highlight the dates discarded in the correlation-based selection. Bottom: temporal coherence of the velocity field. The black rectangle highlights the area of interest for the correlation-based selection.*

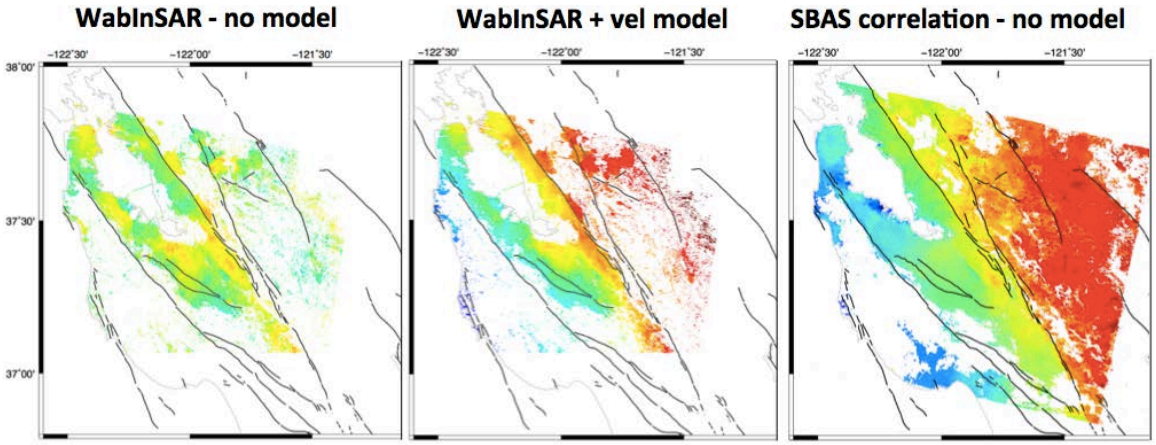

Figure 4: *Comparison between Shirzaei and Bürgmann (2013) velocity maps (using the WabInSAR technique) with long-wavelength signal removed and no GPS model (left) and with a GPS model added (center) and our new correlation-based SBAS velocity map without any model (right).*

strained mostly from a model based on GPS data and InSAR was used only for local deformation (Bürgmann et al., 2000, 2006; Schmidt et al., 2005; Shanker at al., 2011; Shirzaei and Bürgmann, 2013; Shirzaei et al., 2013). Most of these works focused on an earlier time period (up to 2002) with the exception of Shirzaei and Bürgmann (2013) and Shirzaei et al. (2013) who also used the 1992-2011 ERS and Envisat data of track 70 (Figure 4).

To validate our velocity field we follow two steps. First, we compare the line of sight (LOS) estimates of two independent adjacent tracks (70 and 299, Figure 5), which overlap by 4800 km^2. To account for the different viewing geometries of these two tracks we convert the pixels of the two tracks to a common datum using track 70 as a 'master track' and track 299 as a 'slave track' (Ketelaar et al., 2007). In this overlapping area the average difference between the 2 tracks is 0.3 mm/yr confirming that the InSAR velocity maps are consistent and representative of deformation.

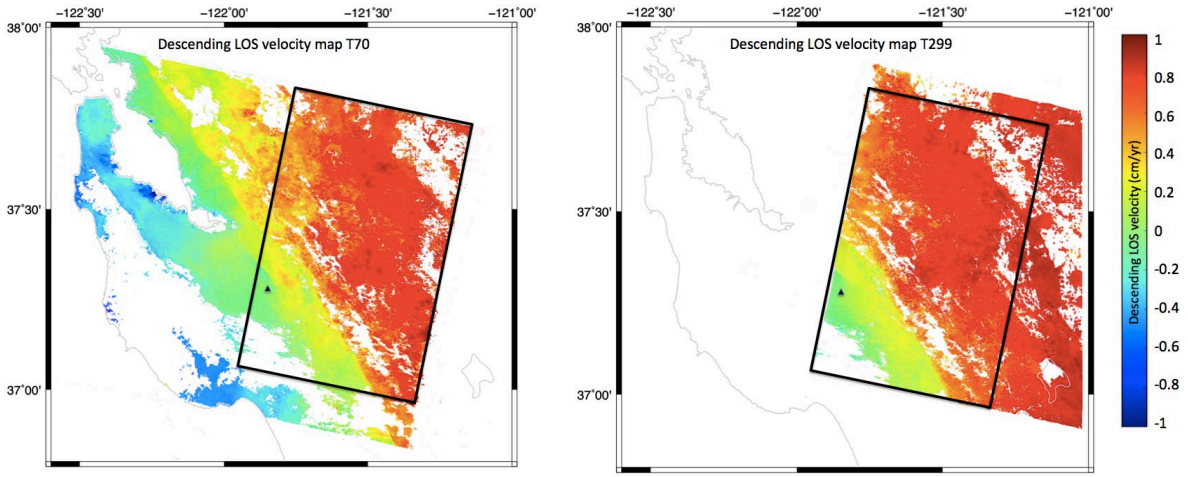

Figure 5: *Comparison between track 70 and 299 LOS velocity maps. In the overlapping area (black rectangle) the average difference is of 0.3 mm/yr. The triangle marks the location of the reference point collocated with the GPS station LUTZ.*

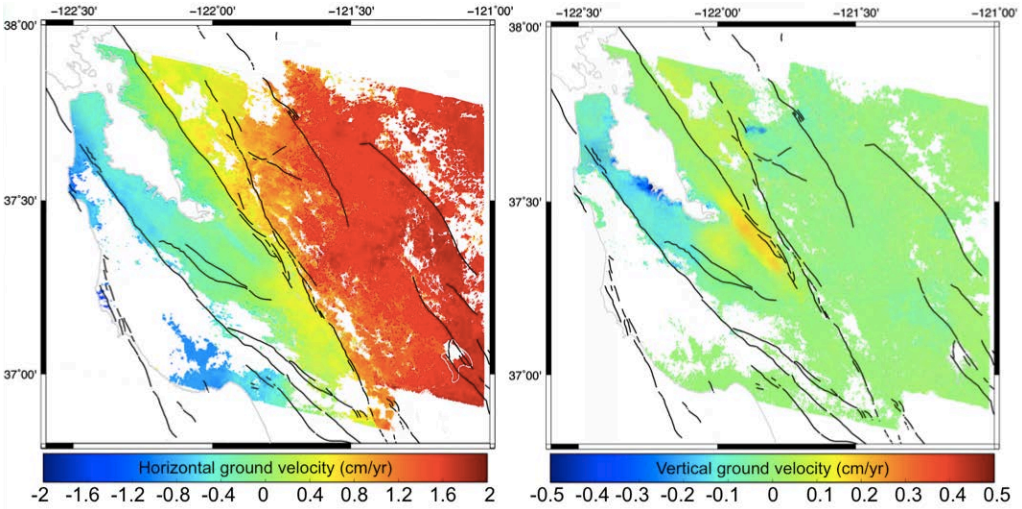

Figure 6: *Mean horizontal (left) and vertical (right) velocity maps obtained by combining ascending and descending viewing geometries.*

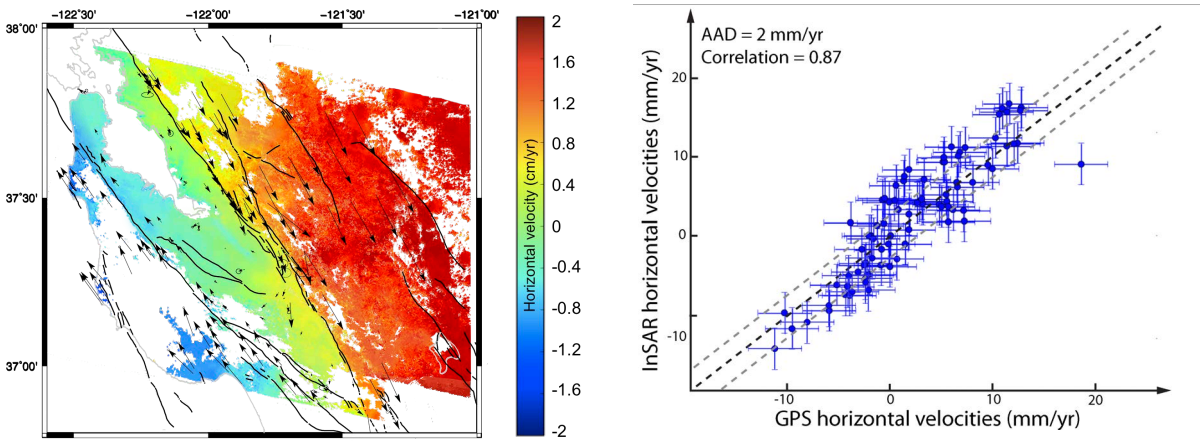

Figure 7: *Comparison between horizontal InSAR and BAVU3 GPS velocities. The average absolute deviation (AAD) between the two is ~ 1 mm/yr.*

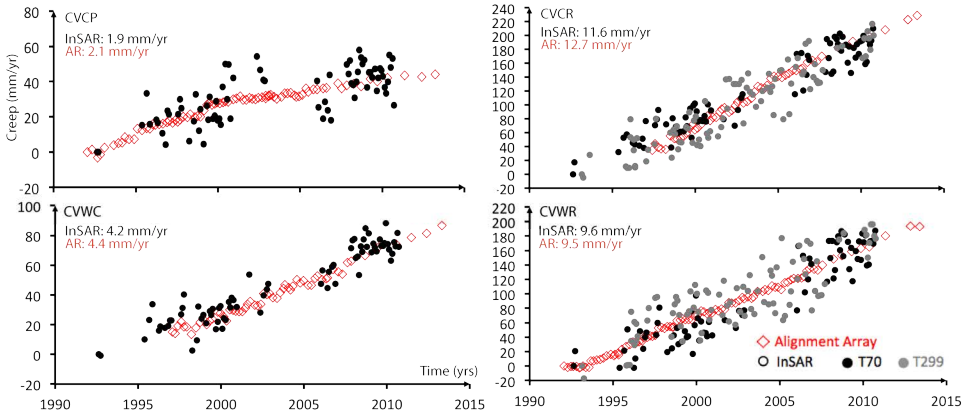

Figure 8: *Example of comparison between the temporal variations of creep detected by InSAR (horizontal velocity) (dots, black and grey for tracks 70 and 299, respectively) and by alignments arrays (red diamonds) on Calaveras Fault.*

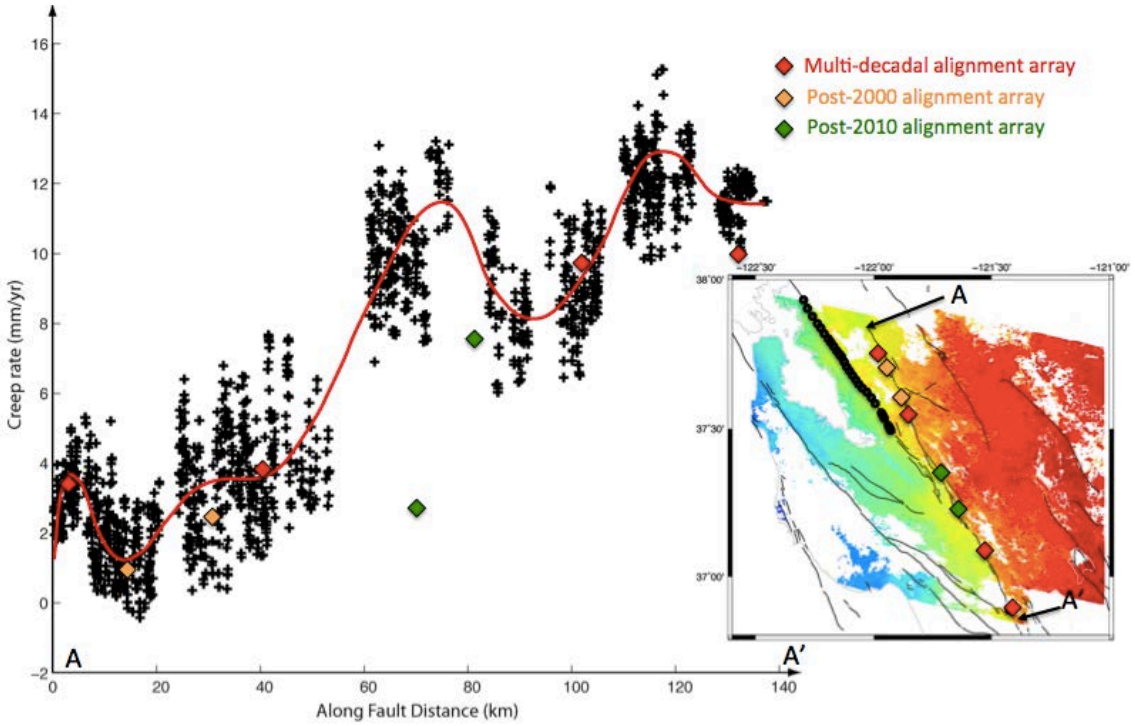

Figure 9: *Along Calaveras creep rate variability (from north, left, to south, right).*

Second we compare our velocity filed with the independent data from BAVU3 GPS and creepmeters and alignment arrays. However, these instruments measure horizontal displacements while InSAR is more sensitive to vertical displacements (due to its incidence angle). Thus, we need to separate the vertical and horizontal components of the LOS InSAR measurements to perform an accurate comparison. To do so we rely on the multiple viewing geometries of the ERS and Envisat satellites (ascending and descending, Figure 2). Because of the different time spans of each track and frames (Table 2) the vertical and horizontal velocity maps (Figure 6) correspond to a mean velocity with a minimum time span of 2003-2011 (track 206) and a maximum time span of 1995-2011 (track 478 frame 747).

The decomposition of LOS InSAR displacements in vertical and horizontal components (Figure 6) confirms that most of the interseismic deformation in the Bay area is horizontal, the vertical deformation being mostly due to hydrological effects near the Santa Clara Valley (Chaussard et al., 2014).

The horizontal velocity map allows for direct comparison with the BAVU3 GPS velocities showing an agreement of ±1 mm/yr (Figure 7). Additionally, InSAR-derived surface creep rates on the Calaveras faults are in good agreement with local creep measurements (Figure 8). We thus demonstrate that InSAR enables resolving vertical and horizontal deformation partitioning in the Bay Area for signals as small as 2 mm/yr over both short and long wavelengths.

Finally, our horizontal velocity map provides new estimates of along-fault creep rate variations for the Calaveras Fault. The creep rate increases from 2 mm/yr in the North to 10-14 mm/yr in the south.

The transition from the slip being partitioned on Calaveras and Hayward in the North (0-60 km) to slip occurring only on Calaveras in the South (60 to 140 km) is clearly marked by a

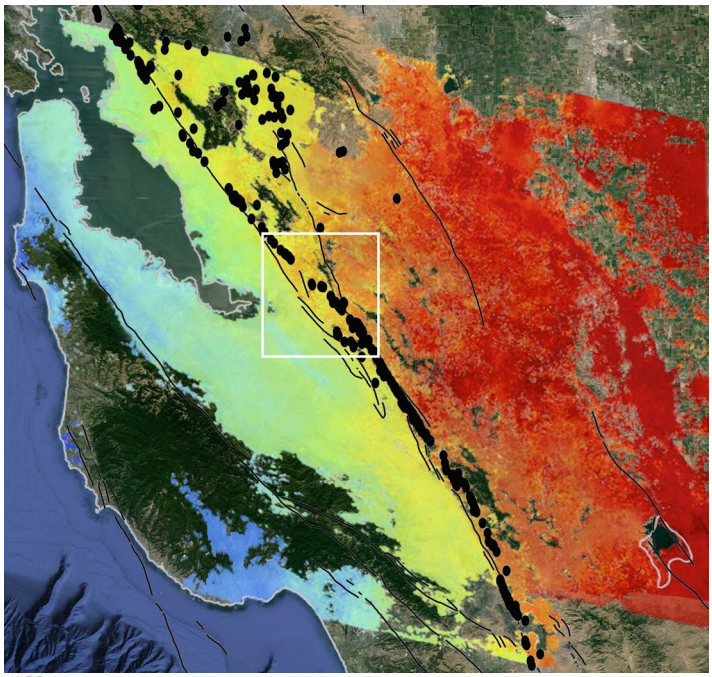

Figure 10: *Horizontal InSAR velocity map overlaying Google Earth imagery. The black lines show the Holocene and historical fault traces and the black dots show the locations of repeating earthquakes. The white rectangle highlights the stepover between the Hayward and Calaveras Faults in the Mission Hills area. In this location the surface creep seems to occur on the Hayward fault (transition from green to yellow colors) while at depth the repeaters are offset toward the east, propagating from the Calaveras fault trace*

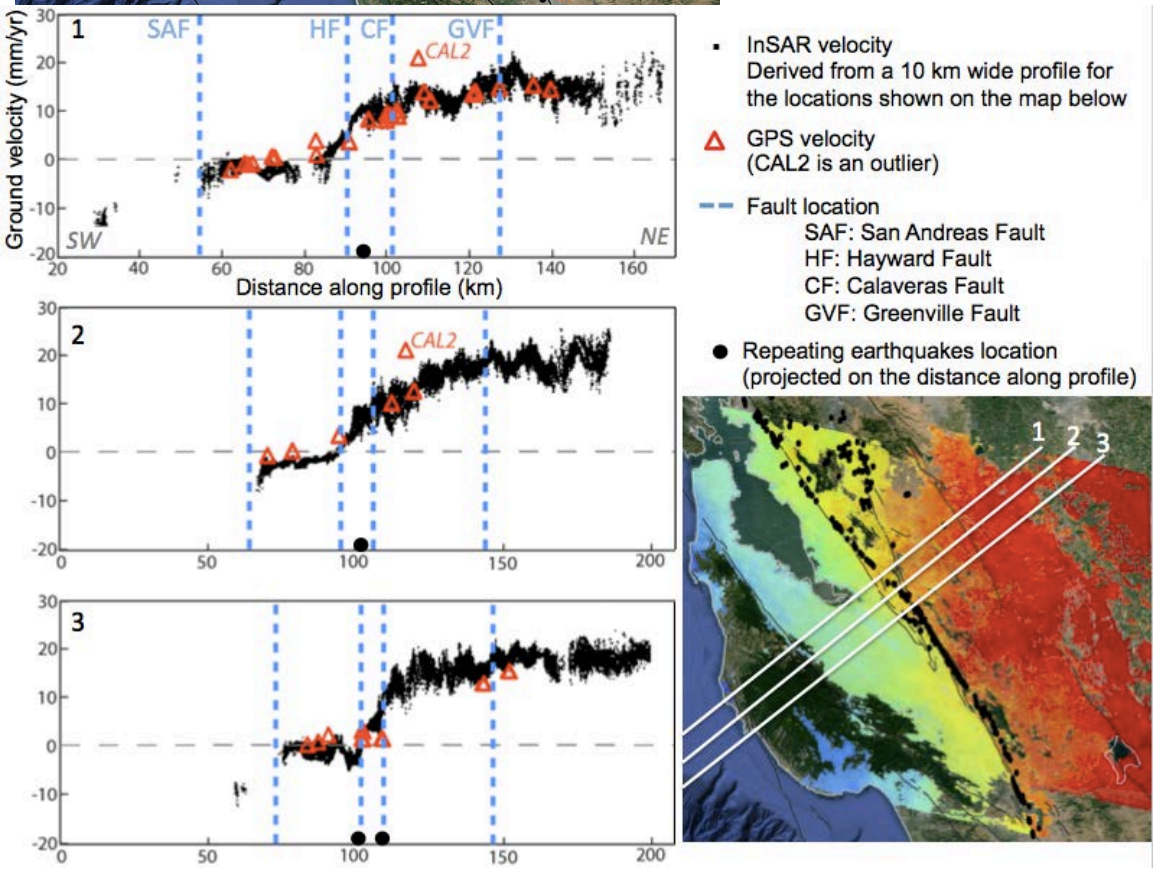

Figure 11:
jump from ~3 to 11 mm/yr of creep at ~60 km. The local variations in creep rate likely reflect different slip distribution with depth that will be investigated in the future with a slip model.

The comparison between the repeating earthquakes locations and the slip distribution reveals a discrepancy at the southern termination of the Hayward Fault (Figure 10). In this location, near Mission Hills, the surface creep continues toward the south on the Hayward Fault, following the geologic fault trace, while the repeating earthquakes are located halfway between the Hayward and Calaveras Fault traces (Figure 10, white rectangle).

Profiles through the stepover (Figure 11) illustrate the migration of the surface creep from Hayward Fault in the North (Profile 2) towards the Calaveras Fault in the South (Profile 4). The repeaters locations for each profile are denoted by a black dot on the x-axis. The surface creep is clearly partitioned between the two faults, while at depth the seismicity and repeaters are essentially continuous. These observations argue for a complex geometry 3D geometry of the stepover and suggest that the Hayward Fault is transitioning from a near-vertical geometry in the north to steeply northeasterly dipping fault that splays off the Calaveras fault in the South, in agreement with Manaker et al. (2005).

C) Repeating Earthquake and Inferred Deep Slip on the Calaveras Fault

The Calaveras fault in the East-Bay lies near major urban areas in the San Francisco Bay region, including San Jose, Fremont, and the cities of the San Ramon Valley corridor, and it has the potential to cause significant loss of life and property. Since 1850, there have been 13 earthquakes of M_L 5 or greater on or near the Calaveras fault. And monitoring of the fault with GPS, creepmeter, gravity, magnetic and seismic data suggest a connection to the Hayward fault with active creep along much of the fault trace. Investigation of the distribution of seismicity along the fault reveals that in regions where $M_L > 5$ earthquakes occur, little seismicity above M_L 1.4 is found and that pre-mainshock and aftershock microseismicity patterns are similar (*Oppenheimer et al*., 1990). This spatial and temporal variability in creep and seismic behavior of the fault suggest that the situation at depth is significantly more complicated than a single locked/creeping region, leading to a time-dependent hazard for the Bay Area

Geodetic measurements of surface deformation provide information on the nature of elastic strain accumulation about seismogenic faults, their locking depth and slip rates, and variations of those parameters in space and time due to time-dependent processes. However, the inference of these properties on fault zones at depth requires various modeling assumptions that are sometimes not well constrained. A primary objective of this project is to help addresses the seismic potential and natural hazard presented by the Calaveras fault in the Eastern San Francisco Bay Area by providing additional constraints on the spatial and temporal distribution of inferred deep fault slip using repeating earthquakes.

Repeating Quakes on the Calaveras

Owing to their occurrence within the fault zone itself, repeating earthquakes provide more direct information on the geometry and time-variability of creep on faults at depth, and for the more complex situation expected within the deep Calaveras fault zone, the addition of repeating earthquake information should help significantly constrain estimates of deep fault strain accumulation. With this in mind we compiled a catalog of characteristically repeating earthquakes (CREs) on the Calaveras fault over an ~ 29.5 year period along an ~85 km long fault section with spatio-temporal coverage that includes the hypocenters of the 1984 Morgan Hill Mw 6.2 and 2007 Alum Rock Mw5.2 earthquakes (Figure 12). There were 236 repeating earthquake se-

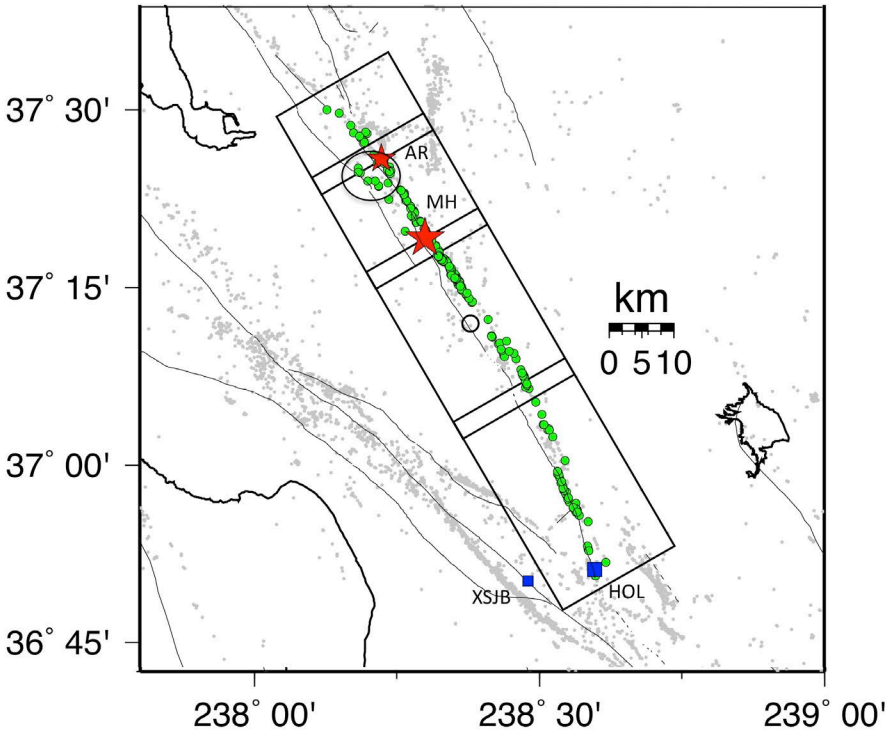

Figure 12: *Locations of 236 repeating earthquake sequences (green/gray circles) identified in the Calaveras fault search area (boxes). These sequences were comprised of 1124 repeating earthquakes occurring during the January 1, 1984 through May 31, 2013 search period. Locations are based the Double-Difference Real Time catalog (Waldhauser and Schaff, 2008; Waldhauser, 2009). Background seismicity > M2.0 are also shown (grey points). 2007 Alum Rock Mw5.2 and 1984 Morgan Hill Mw6.2 are stars labeled AR and MH, respectively. Hollister, CA and XSJB creep meter near San Juan Bautista, CA are squares labeled HOL and XSJB, respectively. Location of Alum Rock Seismic trend is indicated by ellipse containing AR location. Small open circle in center of search area corresponds to 0 km NW in Figure 13.*

quences identified in the region, comprised of 1124 repeating earthquakes occurring during the January 1, 1984 through May 31, 2013 search period.

Results of Deep Creep Rate from Repeaters

One interesting feature of the spatial distribution of the repeating sequences is that a fairly large number occur on what Manaker et al. (2005, see their Fig 10, 12) call the Alum Rock seismic trend just SW of the Alum Rock earthquake (ellipse in Figure 12). A survey view of the repeater inferred slip information for the entire study segment is shown in Figure 13. Inferred deep creep is calculated using the empirical relationship of Nadeau and Johnson (1998). Between -10 to 15 km NW, an initially high and decreasing rate of cumulative creep beginning in 1984 corresponds to the post-seismic slip response of the Calaveras to the 1984 Morgan Hill M6.2 (hypocenter at 13 km NW). The Alum Rock trend of repeaters appears as the southwest splay between 20 to 30 km NW in map view. As this study progresses, it will be interesting to see what kind of slip behavior this and other secondary structures have. We will also look at a number of cross-sections of the relocated repeating and non-repeating seismicity stepping along the fault to further illuminate other structural discontinuities and how deep fault slip is partitioned on these structures.

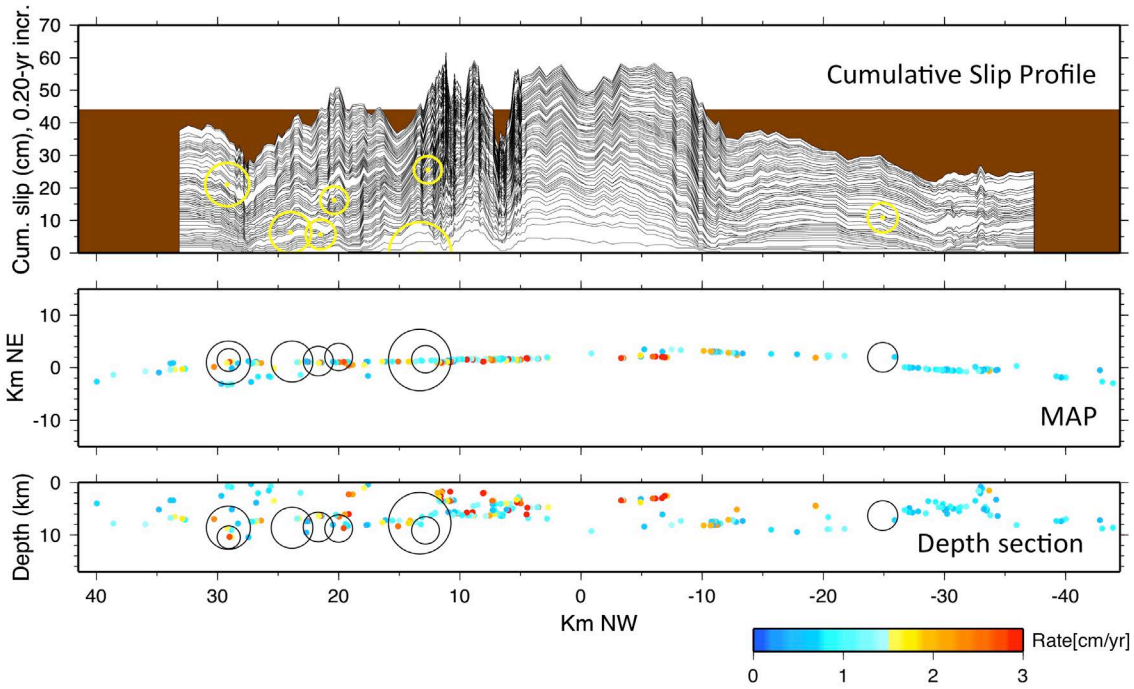

Figure 13: *(top) along fault, cumulative creep contours taken every 0.2 years since the beginning of 1984, smoothed over 15 sequences and stepped every 1 sequence along strike. Brown is cumulative creep assuming a 1.5 cm/yr rate for the 29.414 year period. Yellow circles are M >4.5 earthquakes plotted at along fault locations and cumulative slip-time. (middle) Along fault locations of REQ sequences colored by average creep rate over the entire study period (color scale at bottom). Large black circles are M>4.5 events corresponding to the yellow circles at top. (Bottom) Same as middle but in along fault depth section. Large circles located at 13 km NW in each panel corresponds to the 1984 Morgan Hill M6.2 earthquake hypocenter.*

This information will also be combined with InSAR, GPS and other diverse geodetic datasets to provide improved constraints for a kinematic model of the variability of interseismic creep on the Calaveras fault. The goals of the modeling effort are to better delineate creeping zones on the Calaveras fault and their rates through time, to detect previously unknown transient slip events and to better characterize known events, such as postseismic slip following the 2007 Alum Rock earthquake.

References

Bürgmann, R., G. Hilley, A. Ferretti, and F. Novali (2006), Resolving vertical tectonics in the San Francisco Bay Area from permanent scatterer InSAR and GPS analysis, Geology, 34(3), 221–224, doi:10.1130/G22064.1.

Burgmann, R., Schmidt, D. A., Nadeau, R. M. M., d'Alessio, M., Fielding, E. J., Manaker, D., et al. (2000). Earthquake potential along the northern Hayward fault, California. *Science*, *289*(5482), 1178–1182. doi:10.1126/science.289.5482.1178

Chaussard, E., R. Bürgmann, M. Shirzaei, E. J. Fielding, and B. Baker (2014), Predictability of hydraulic head changes and characterization of aquifer-system and fault properties from In-

SAR-derived ground deformation, J. Geophys. Res. Solid Earth, 119, 6572–6590, doi:10.1002/2014JB011266.

d'Alessio, M. A., I. A. Johanson, R. Bürgmann, D. A. Schmidt, and M. H. Murray (2005), Slicing up the San Francisco Bay Area: block kinematics and fault slip rates from GPS-derived surface velocities, J. Geophys. Res., 110(B06403), doi:10.1029/2004JB003496.

Fattahi, H., and F. Amelung (2014). InSAR uncertainty due to orbital errors. *Geophysical Journal of the Royal Astronomical Society*, *199*(1), 549–560. doi:10.1093/gji/ggu276

Funning, G. J., R. Bürgmann, A. Ferretti, F. Novali, and A. Fumagalli (2007), Creep on the Rodgers Creek fault, northern San Francisco Bay area from a 10 year PS-InSAR dataset, Geophysical Research Letters, 34(19), L19306, doi:10.1029/2007GL030836.

Johanson, I. A., and R. Bürgmann (2005), Creep and quakes on the northern transition zone of the San Andreas fault from GPS and InSAR data, Geophysical Research Letters, 32(14), doi:10.1029/2005GL023150.

Johanson, I. A., E. J. Fielding, F. Rolandone, and R. Bürgmann (2006), Coseismic and Postseismic Slip of the 2004 Parkfield Earthquake from Space-Geodetic Data, Bull. Seismol. Soc. Am., 96(4B), S269–S282, doi:10.1785/0120050818.

Johnson, K. M. (2006), Frictional Properties on the San Andreas Fault near Parkfield, California, Inferred from Models of Afterslip following the 2004 Earthquake, Bull. Seismol. Soc. Am., 96(4B), S321–S338, doi:10.1785/0120050808.

Jolivet, R., R. Bürgmann, and N. Houlié (2009), Geodetic exploration of the elastic properties across and within the northern San Andreas Fault zone, Earth and Planetary Science Letters, 288(1-2), 126–131, doi:10.1016/j.epsl.2009.09.014.

Ketelaar, G., Van Leijen, F., Marinkovic, P., and Hanssen, R. F. (2007). Multi-track PS-InSAR datum connection, H. Lacoste, L. Ouwehand (Eds.), ENVISAT Symposium 2007, ESA.

Manaker, D. M., R. Bürgmann, W. H. Prescott, and J. Langbein (2003), Distribution of interseismic slip rates and the potential for significant earthquakes on the Calaveras fault, central California, J. Geophys. Res., 108(B6), 2287.

Manaker, D. M., A. J. Michael, and R. Burgmann, (2005). Subsurface structure and kinematics of the Calaveras-Hayward fault stepover from three-dimensional V-P and seismicity, San Francisco Bay region, California. Bulletin of the Seismological Society of America, 95(2), 446–470. doi:10.1785/0120020202

Marinkovic, P. and Y. Larsen (2013). Consequences of long-term ASAR lo- cal oscillator frequency decay—an empirical study of 10 years of data, European Space Agency, in Proceedings of the Living Planet Symposium (abstract), Edinburgh, U. K

Murray, M. H., and P. Segall (2001), Modeling broadscale deformation in northern California and Nevada from plate motions and elastic strain accumulation, Geophysical Research Letters, 28(22), 4315–4318.

Nadeau, R. M., and L. R. Johnson, (1998) Seismological Studies at Parkfield VI: Moment Release Rates and Estimates of Source Parameters for Small Repeating Earthquakes, Bull. Seismol. Soc. Amer., 88, 790-814,

Oppenheimer, D.H., W. H. Bakun and A. G. Lindh (1990) Slip Partitioning of the Calaveras Fault, California, and Prospects for Future Earthquakes. J. Geophys. Res, 95(B6), 8483-8498.

Parsons, T. (2002), Post-1906 stress recovery of the San Andreas fault system calculated from three-dimensional finite element analysis, Journal of Geophysical Research, 107(B8), 2162, doi:10.1029/2001JB001051.

Pollitz, F. (2004), A physical model for strain accumulation in the San Francisco Bay region: Stress evolution since 1838, Journal of Geophysical Research, 109(B11), B11408–, doi:10.1029/2004JB003003.

Pollitz, F. F., and M. Nyst (2004), A physical model for strain accumulation in the San Francisco Bay Region - Pollitz - 2004 - Geophysical Journal International - Wiley Online Library, Geophys. J. Int.

Prescott, W. H., J. C. Savage, J. L. Svarc, and D. Manaker (2001), Deformation across the Pacific-North America plate boundary near San francisco, California, J. Geophys. Res., 106(B4), 6673–6682.

Ryder, I., and R. Bürgmann (2008), Spatial variations in slip deficit on the central San Andreas Fault from InSAR - Ryder - 2008 - Geophysical Journal International - Wiley Online Library, Geophys. J. Int., 175(3), 837–852.

Savage, J. C. (2004), Strain accumulation across the Coast Ranges at the latitude of San Francisco, 1994–2000, Journal of Geophysical Research, 109(B3), B03413–, doi:10.1029/2003JB002612.

Schmidt, D. A., R. Bürgmann, R. M. Nadeau, and M. d'Alessio (2005), Distribution of aseismic slip rate on the Hayward fault inferred from seismic and geodetic data, J. Geophys. Res., 110(B8), doi:10.1029/2004JB003397.

Shanker, P., F. Casu, H. A. Zebker and R. Lanari (2011). Comparison of Persistent Scatterers and Small Baseline Time-Series InSAR Results: A Case Study of the San Francisco Bay Area. IEEE Geoscience and Remote Sensing Letters, 8(4), 592–596. doi:10.1109/LGRS.2010.2095829

Shirzaei, M., and R. Bürgmann (2013), Time‐dependent model of creep on the Hayward fault from joint inversion of 18 years of InSAR and surface creep data, Journal of Geophysical Research.

Shirzaei, M., R. Burgmann and T. Taira (2013). Implications of recent asperity failures and aseismic creep for time-dependent earthquake hazard on the Hayward fault. Earth and Planetary Science Letters, 371-372(C), 59–66. doi:10.1016/j.epsl.2013.04.024

Waldhauser, F., and D. P. Schaff (2008) Large-scale relocation of two decades of Northern California seismicity using cross-correlation and double-difference methods, J. Geophys. Res., 113, B08311, doi:10.1029/2007JB005479.

Waldhauser, F. (2009) Near-real-time double-difference event location using long-term seismic archives, with application to Northern California, Bull. Seism. Soc. Am., 99, 2736-2848, doi:10.1785/0120080294.

Wright, T. J., B. E. Parsons and Z. Lu (2004). Toward mapping surface deformation in three dimensions using InSAR. Geophysical Research Letters, 31(1). doi:10.1029/2003GL018827